Received: 22 May 2020 | Revised: 12 July 2020 | Accepted: 15 July 2020
DOI: 10.1002/qua.26423

FULL PAPER

International Journal of QUANTUM CHEMISTRY WILEY

Rapid computational evaluation of small-molecule hydrolase mimics for preorganized H-bond networks

Alara Öner | Nihan Çelebi-Ölçüm

Department of Chemical Engineering, Yeditepe University, Istanbul, Turkey

Correspondence
Nihan Çelebi-Ölçüm, Department of Chemical Engineering, Yeditepe University.
Email: nihan.celebi@yeditepe.edu.tr

Funding information
Türkiye Bilimsel ve Teknolojik Araştırma Kurumu (TUBITAK), Grant/Award Number: 116Z514

Abstract

Spirocyclic oligomers formed by coupling chiral cyclic building blocks carrying the catalytic machinery of hydrolases (spiroligozymes) catalyze the transesterification of vinyl trifluoromethylacetate with methanol but suffer from the lack of enzyme-like preorganization of their catalytic functionalities in a well-defined geometry via H-bond networks. The computational protocol presented herein combines different levels of theories to rapidly explore structural modifications for an improved structural preorganization. Calculations predict that a modification as simple as replacing the five-membered building block holding the alcohol moiety with a six-membered analog in spiroligozymes significantly increases the occupancy of the H-bond between the benzyl alcohol-pyridine nucleophilic dyad that mimics the Ser-His-Asp/Glu triad of hydrolases. The computed energy profile is indicative of faster acylation of this derivative compared to the parent spiroligozyme and highlights the importance of inclusion of an oxyanion hole motif for efficient catalysis.

KEYWORDS
DFT, enzyme mimics, molecular dynamics, Organocatalysis, transesterification

1 | INTRODUCTION

Enzymes are macromolecular biocatalysts that accelerate chemical reactions, allowing metabolic processes to occur at rates fast enough to sustain life.[1] Besides carrying out reactions to maintain our metabolism, enzymes are increasingly used as environmentally friendly catalysts in the chemical industry.[2–5] Essentially, enzymatic transesterification has been widely explored for biodiesel production, presenting several advantages over chemical catalysts, one of the most important being mild reaction conditions.[6] As important green alternatives to biocatalysts, small organic molecules can effectively mimic functional group richness of enzymes within a much simpler molecular framework.[7–20] The interest in grafting catalytic active sites of enzymes onto organocatalytic scaffolds led to the development of new transesterification catalysts, called "spiroligozymes", by placing the catalytic machinery of hydrolase enzymes onto modular spiro-fused bispeptides with the help of quantum mechanical transition state (TS) calculations using the "inside-out" approach.[20] Hydrolases use a proton shuttle mechanism between serine, histidine, and aspartate/glutamate residues[21] engaged in a tightly maintained H-bond network[22–24] to activate serine as a nucleophile to initiate its attack on the substrate (Figure 1).[25] The Ser-His-Asp/Glu nucleophilic triad of a hydrolase is mimicked with an alcohol-pyridine dyad in spiroligozymes (Figure 1). The best spiroligozyme increased the rate of the transesterification reaction between vinyl trifluoromethylacetate and methanol by 2200-fold for the acylation step and 130-fold for the deacylation step.[20] However, calculations demonstrated that, in contrast to the high-level structural and electrostatic preorganization observed in naturally evolved enzymes,[26] the catalytic groups in spiroligozymes sample numerous alternative conformations beside the active one, and the H-bond network required for efficient catalysis is not maintained. These computational results suggest that the activities of spiroligozymes can be significantly improved by providing a high-level preorganization of the catalytic functional groups.

In this article, we report a rapid computational evaluation protocol to assess the structural modifications that may result in rate enhancements due to an increased H-bond network stability in small-molecule catalysts, which constitutes an important step toward the design of organocatalysts

https://doi.org/10.1002/qua.26423

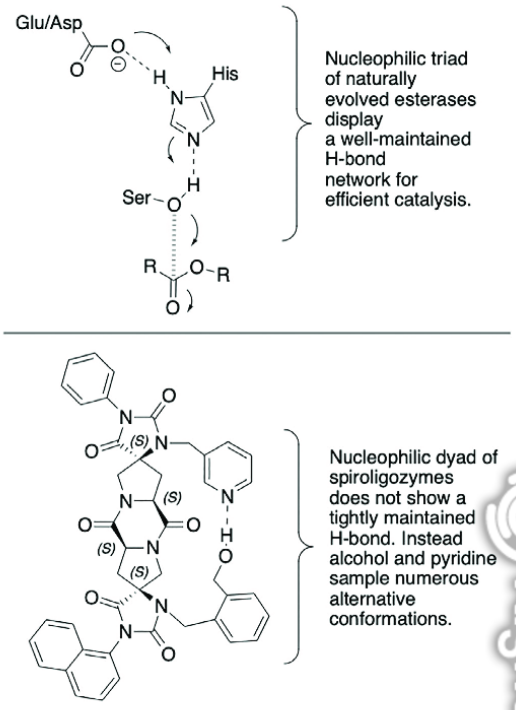

FIGURE 1 Catalytic functional groups of naturally evolved esterases and spiroligozymes developed using the "inside-out" approach[20]

presenting catalytic functionalities in a well-defined arrangement forming an enzyme-like active site for efficient catalysis. Application of the proposed protocol to the parent bifunctional spiroligozyme shown in Figure 1 identified derivatives with an improved occupancy of the H-bond between benzyl alcohol and pyridine essential for catalysis.

2 | METHODS

Figure 2 summarizes the applied computational protocol for the identification of structural modifications that will result in increased H-bond occupancy in an organocatalytic framework. The protocol starts with the generation of synthesizable derivatives of the parent molecule. For this purpose, MedChem Transformations, an approach that applies predefined transformation rules by a match-and-replace algorithm to existing ligands to obtain new chemical structures, was used as implemented in MOE.[27] A total of 175 reactions is defined in the default library.

The second step of the protocol involves a fast conformational analysis for each generated derivative unless the transformation changed the catalytic functional groups (pyridine and alcohol) in the parent molecule. The conformational search was carried out using MOE with MMFF94x, setting the energy convergence criterion to a root mean square gradient smaller than 0.001 kcal mol^{-1} Å^{-2}. MMFF94x is an all-atom forcefield, parametrized for small organic molecules, modified from MMFF94s[28] to force conjugated nitrogens planar. The solvent effects were implicitly taken into account using the Generalized Born solvation model[29] using an exterior dielectric constant, ε = 4.81, representing chloroform. A LowModeMD sampling procedure[30,31] was used that performs molecular dynamics (MD) perturbations along low-frequency vibrational modes. A LowModeMD search was selected for its ability to explore conformations near the relevant and realistic low-energy states and for its efficiency in locating most of the local minima of arbitrarily complex multicomponent systems.[31] An iteration limit of 1000 with a rejection limit of 100 was used in order to obtain a sufficient sample of conformational minima for initial evaluation in a reasonable amount of time.[32] Two conformations having a root mean square distance less than 0.25 were considered duplicates. Conformations with ΔE > 7 kcal mol^{-1} relative to the lowest-energy conformer (ΔE_{MM}) were discarded. The Boltzmann populations were calculated according to the formula

$$\text{MM Population} = \frac{e^{-\Delta E_{MM}/k_B T}}{\sum\left(e^{-\Delta E_{MM}/k_B T}\right)} \times 100$$

FIGURE 2 Computational protocol

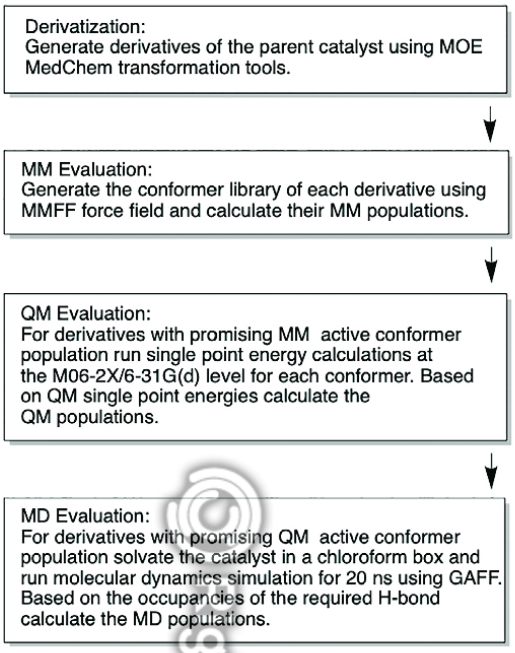

where ΔE_{MM} is the difference between the energy of the conformer of interest and the energy of the global minimum conformation obtained from molecular mechanics (MM) force field calculations, T is the absolute temperature, and k_B is the Boltzmann constant. The resulting conformer libraries were first examined for the population of the conformers with the required H-bond between the catalytic dyad. An N···H—O H-bond distance cut-off of 3 Å was applied as the selection criterion for an initial filtering. Conformers with $d_{N\cdots H-O}$ < 3 Å were considered in group **H-Bond**, as the others were grouped as **No-H-Bond**. Derivates with **H-Bond** MM population higher than 50% were then clustered into three groups based on the N···H—O distance and the orientation of the substrate upon alignment of the catalytic dyad with the quantum mechanically optimized active site model (QM theozyme) (Figure 3).

The first cluster, called **Active-H-Bond**, is composed of conformers in which the arrangement of the pyridine-alcohol hydrogen bond with respect to the chiral backbone of the spiroligozyme resulted in an exposed oxygen nucleophile. The second cluster, called **Inactive-H-Bond**, includes conformers with a buried oxygen nucleophile that requires the approach of the substrate from the hindered face of the dyad. Conformers with $d_{N\cdots H-O}$ < 3 Å, yet having an angle less than 120° between the plane of pyridine and N···H—O, were also considered in this group. Cluster **No-H-Bond** includes all other conformers, in which the arrangement of the two catalytic functional groups does not allow a H-bonding interaction between pyridine and alcohol. The population of each cluster was deduced as the sum of the individual conformer populations in the cluster.

The derivatives with **Active-H-Bond** MM population greater than the population of other clusters were subjected to quantum mechanical (QM) evaluation. For each selected derivative, energies of all conformers, regardless of their population, were refined using single-point energy calculations with density functional theory at the M06-2X/6-31G(d) level.[33] The calculations were performed in a dielectric continuum representing chloroform as the solvent using the integral-equation-formalism polarizable continuum model (IEF-PCM)[34–36] with radii and non-electrostatic terms for the SMD solvation model.[37] All quantum mechanical calculations were performed using Gaussian 09.[38] QM populations of conformers were determined using the Boltzmann distribution

$$\text{QM Population} = \frac{e^{-\Delta E_{QM}/k_B T}}{\sum\left(e^{-\Delta E_{QM}/k_B T}\right)} \times 100$$

where ΔE_{QM} *is* the relative energy of the conformer of interest and the minimum energy conformer obtained from QM calculations, T is the absolute temperature, and k_B is the Boltzmann constant. The populations of the clusters were updated with the QM populations. Derivatives with **Active-H-Bond** QM population greater than the population of other clusters were taken into consideration for molecular dynamics (MD) evaluation.

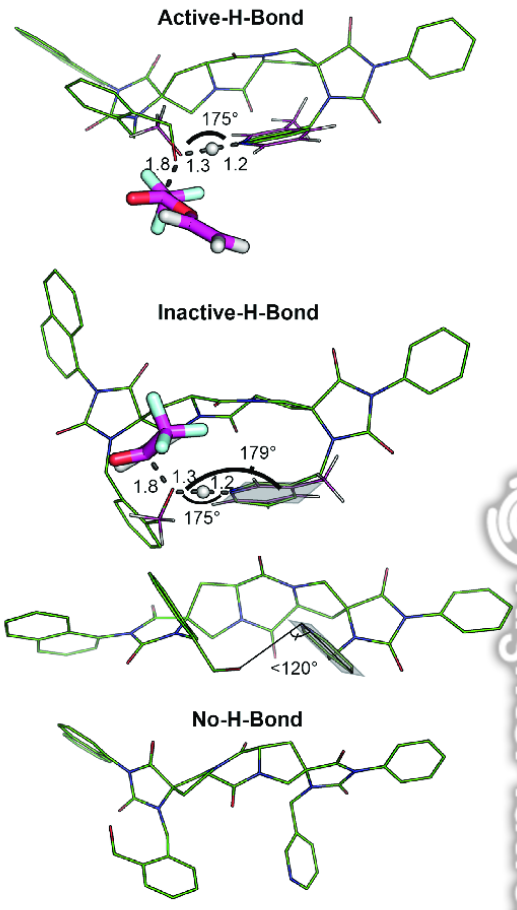

FIGURE 3 Representative conformer structures of spiroligozymes (green lines) in each cluster based on orientation of the substrate (vinyl trifluoromethylacetate, magenta sticks) upon alignment of the catalytic dyad with the quantum mechanically optimized transition state model (QM theozyme, magenta lines with key distances in Å and angles in degrees)

MD simulations were performed using AMBER 12[39] to evaluate the occupancy of the H-bond between the catalytic dyad in a dynamic explicitly solvated environment. The antechamber module of AMBER 12 was used to generate the spiroligozyme parameters using the general Amber forcefield (GAFF),[40] with partial charges set to fit the electrostatic potential computed at HF/6-31G(d) by RESP.[41,42] The Merz-Singh-Kollman scheme[43,44] was used to calculate the charges using Gaussian 09.[38] Spiroligozymes were placed in a chloroform box[45] with a solvent layer of at least 10 Å around the solute. Initially, only the solvent molecules were relaxed, followed by an unrestrained minimization of all atoms. The systems were then heated in six 50 K, 50 ps steps to 300 K with a 1-fs time step at constant-volume periodic boundary conditions using a harmonic restraint of 10 kcal mol^{-1} to the spiroligozyme. The temperature was controlled and equalized using the Langevin equilibration scheme. Each system was equilibrated for 2 ns with a 2-fs time step at constant volume and another 2 ns at a constant pressure of 1 atm. A 20-ns production run was performed using the isothermal-isobaric ensemble (NPT). Long-range electrostatic interactions were treated with the particle mesh-Ewald method.[46] Trajectories were saved at every 10 ps, resulting in a total of 2000 frames. The trajectories were analyzed using the ptraj module of AMBER 12. H-bond occupancy defines the cumulation of MD snapshots in the H-bond region ($d_{N\cdots H\text{-}O} < 3.5$ Å & $120° < \theta_{N\cdots H\text{-}O} < 180°$). This region is indicated with a blue rectangle on the corresponding N···H—O distance-angle scatter plots, and MD population is calculated as the percentage of the number of frames in the H-bond region with respect to the total number of frames in the simulation. This MD evaluation protocol successfully predicted the active and inactive enzyme designs for Kemp elimination on the basis of the stability of the required H-bond networks in the active site[26] and was previously used for the parent spiroligozymes in the this study to assess whether the H-bond between the dyad was maintained in a solvated dynamic environment.[20] In order to avoid false-positive conclusions,[47] six replicas for each system were performed. All results are given in the SI, and one of the representative simulations is illustrated in the text.

Finally, the energy profile of the acyl transfer reaction from vinyl trifluoromethylacetate to methanol was constructed using density functional theory in the presence of the most promising spiroligozyme derivative as a catalyst. All stationary points were located using Gaussian 09[38] at the

M06-2X/6-31G(d)[33] level of theory in a dielectric continuum representing chloroform using the IEF-PCM[34–36] with radii and nonelectrostatic terms for the SMD[37] solvation model. The M06-2X density functional method was chosen for its good performance for thermochemical kinetics and for the treatment of noncovalent interactions.[33] Frequency calculations were used to characterize the stationary points as first-order saddle points or minima. Corrections in enthalpy and free energy, including zero-point vibrational energies, were calculated using the harmonic oscillator approximation at 298.15 K for 1 M standard state. Minimum energy paths were followed from the transition states both in the reverse and forward directions using the intrinsic reaction coordinate (IRC) method.[48,49]

3 | RESULTS AND DISCUSSION

Esterases catalyze the hydrolysis of carboxyl esters using a proton shuttle mechanism between Ser-His-Asp/Glu catalytic triad for the activation of an alcohol nucleophile that initiates the catalytic cycle by covalently binding to the substrate (Figure 1).[21] Their high efficiency is attributed to the high-level structural and electrostatic preorganization with tightly maintained H-bonds in their active sites.[22–24] Catalytic spiroligomers (called spiroligozymes) were constructed by coupling cyclic, sterochemically pure building blocks carrying alcohol and pyridine functional groups to mimic the Ser-His-Asp/Glu nucleophilic triad of natural hydrolases so that the resulting spiroligomer scaffolds with fused ring structures are capable of presenting these catalytic functional groups in a three-dimensional arrangement as suggested by quantum mechanically optimized transition state models (QM theozyme) (Figure 4).[20] Modeling based on the **TS dyad** suggested that spiroligozyme **A** could approximate the three-dimensional (3D) arrangement of catalytic functional groups depicted in the theozyme (Figure 4). Indeed, kinetic experiments using vinyl trifluoromethylacetate as the substrate showed that the rate of acylation of **A** is 250-fold faster than the rate of acylation of the control spiroligomer, displaying a phenyl group instead of a pyridyl group.[20] However, high-level QM calculations and analysis of MD trajectories revealed that the required H-bonding interaction between the catalytic dyad for the proton shuttle mechanism for activating the alcohol as nucleophile is not maintained in designed spiroligozymes. Based on these computational observations,[20] we applied the proposed computational protocol to spiroligozyme **A**, with the aim of identifying structural modifications that could increase the H-bond occupancy of the catalytic dyad by possibly destabilizing alternative unproductive conformations. We selected bifunctional spiroligozyme **A** as the parent compound to be able to focus on the preorganization of the nucleophilic dyad and to understand the importance of the presence of the oxyanion hole, another catalytic motif present in hydrolases[50–52] (see the SI) previously modeled in trifunctional spiroligozymes.[20] All steps of the same computational protocol were applied to the parent compound **A** for comparison, and the results are tabulated in the corresponding tables.

3.1 | Derivatization

Most of the computational design approaches based on existing molecular structures are faced with significant synthetic challenges as synthetic routes to predicted favorable modifications usually are not known. To overcome this challenge, a derivatization tool that uses a library of 175 transformations commonly applied in medicinal chemistry was used. The derivatization of the parent spiroligozyme **A** using the MedChem transformation tool in MOE gave 116 distinct derivatives. A complete list of derivatives and the corresponding transformation rules are given in the SI. A total of 42 derivatives involve modifications in the catalytic functional groups (alcohol or pyridine) and are therefore not considered for further evaluation.

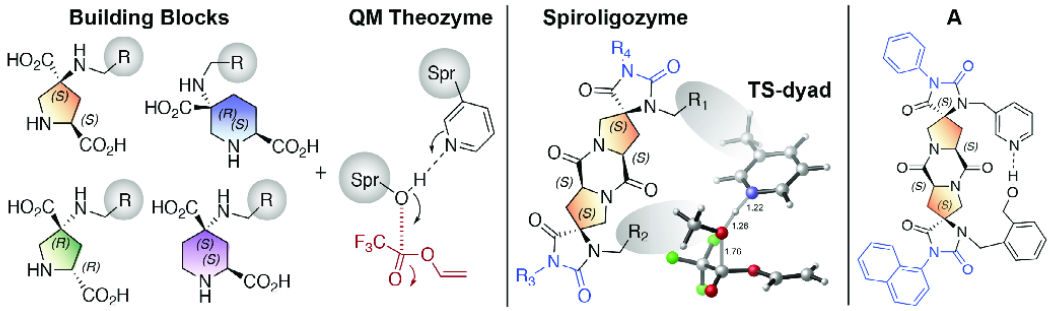

FIGURE 4 Design of bifunctional spiroligozymes[20]

3.2 | MM evaluation

A total of 74 derivatives were subjected to MM evaluation. The number of conformers obtained for each derivative upon fast initial conformational analysis varies between 150 and 450 (see the SI).[32] The conformer library of each derivative was sorted in the order of increasing N···H—O distance between the dyad. As an initial filter, conformers with $d_{N\cdots H-O}$ < 3 Å were considered H-bonded (**H-Bond**), whereas all other conformers were listed as **No-H-Bond**.[53] A total of 10 derivatives with **H-Bond** MM population greater 50% were selected for extended analysis (Table 1).

The angle between the plane of pyridine and N···H—O was determined for all individual conformers with $d_{N\cdots H-O}$ < 3 Å for the selected derivatives (see the SI). As the lone pair of nitrogen is in the plane of pyridine, a planar geometry is indicative of a stronger H-bonding interaction and is essential for proton transfer. A 120° cut-off was applied, and conformers with an N···H—O out-of-plane interaction of pyridine were considered in the **Inactive-H-Bond** cluster. Other conformers with $d_{N\cdots H-O}$ < 3 Å were aligned with the theozyme to assess the extent to which the oxygen nucleophile is exposed to the substrate in the current conformational arrangement and the agreement with the optimal transition state geometry. Conformers with a buried oxygen nucleophile that requires the approach of the substrate from the hindered face of the dyad are in the **Inactive-H-Bond** cluster. The **Active-H-Bond** cluster includes the conformers with an exposed oxygen nucleophile. Table 1 summarizes the MM populations of the selected 10 derivatives.

Although 9 of 10 derivatives have an **Active-H-Bond** MM population greater than that of the parent compound **A**, for 5 of the selected derivatives, the conformations that do not allow the optimum geometry required for the acylation step are energetically favored, and the population of the **Inactive-H-Bond** cluster is higher than the population of other clusters. The derivatives with a higher **Active-H-Bond** MM population compared to the other clusters (Table 1, denoted by *) are selected to proceed to the QM evaluation step.

Figure 5 shows how the structures of these derivatives differ from that of the parent molecule. **A** is composed of two five-membered building blocks with (*S*),(*S*) configuration, each holding one of the catalytic functional groups of the nucleophilic dyad. **D20** results from a ring expansion in

TABLE 1 MM populations of selected derivatives

Derivative no.[a]	No. of conformers	Active-H-bond (%)	Inactive-H-bond (%)	No-H-bond (%)
A	236	13	6	81
4*	341	35	35	30
6	268	20	41	39
20*	256	84	0	16
21	182	16	68	16
22	152	25	59	16
31*	362	52	2	45
34*	251	73	1	26
35*	204	88	2	9
56	195	5	59	36
59	305	25	25	49

[a]Derivatives denoted by * are selected for QM evaluation.

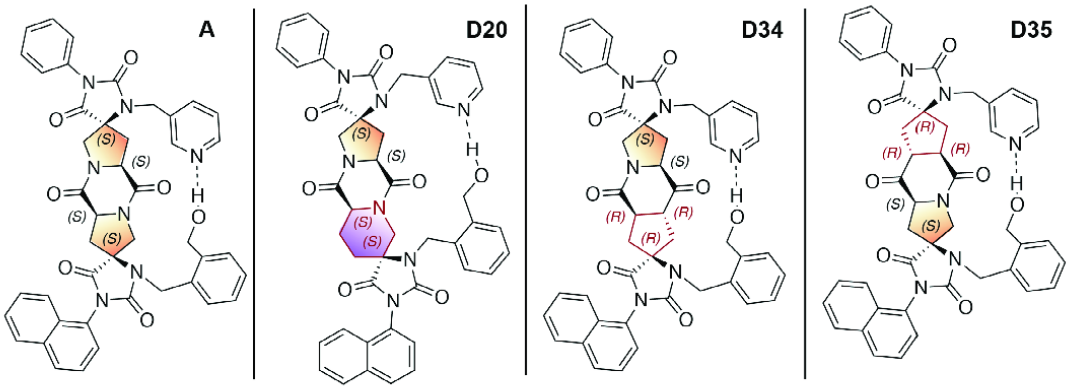

FIGURE 5 Most promising derivatives according to MM and QM evaluations. The modifications are shown in red

the five-membered building block carrying the alcohol moiety to a six-membered building block with the same stereochemical information. **D34** and **D35** are obtained by the amide-to-ketone transformation rule and involve the saturation of the ring nitrogen in each of the building blocks, holding pyridine and alcohol, respectively. This results in a new stereocenter in place of the peptide bond formed from their coupling. The nature of these transformations suggests a possible relief in the backbone strain caused by the arrangement of the catalytic functionalities upon formation of the H-bond. MM evaluation predicts derivatives **D20**, **D34**, and **D35** as the most promising, having an **Active-H-Bond** MM population greater than 70%. **Inactive-H-Bond** conformations are significantly disfavored in these derivatives, and the lowest-energy **No-H-Bond** conformer is 1.3 to 1.8 kcal mol^{-1} higher in energy than the global minimum, which is an **Active-H-Bond** conformer (see the SI). The individual populations of the lowest-energy conformers are 41%, 46%, and 42% for **D20**, **D34**, and **D35,** respectively.

3.3 | QM evaluation

Based on the MM evaluation results, five derivatives were subjected to QM evaluation. QM populations of the selected derivatives are summarized in Table 2. The geometries of the lowest-energy conformer of each cluster and their energies with respect to the global minimum are given in Figure 6.

TABLE 2 QM Populations of Selected Derivatives

Derivative no.[a]	No. of conformers evaluated	Active-H-bond (%)	Inactive-H-bond (%)	No-H-bond (%)
A	236	8	0	92
4	341	0	96	4
20*	256	77	0	23
31	362	2	91	7
34*	251	100	0	0
35*	204	61	36	2

[a]Derivatives denoted by * are selected for MD evaluation.

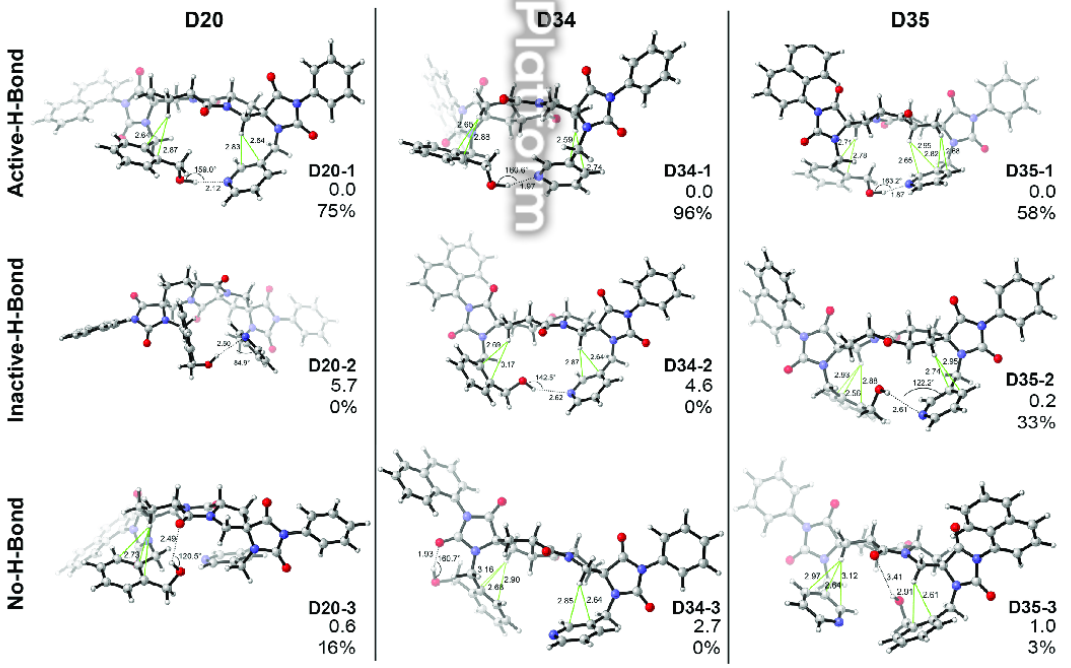

FIGURE 6 Geometries, relative energies (kcal mol^{-1}), and individual populations of the lowest-energy conformers in each cluster of promising derivatives based on QM evaluation

Even though assessing the strength of an H-bond is difficult and depends on many parameters, it is generally accepted that the shorter the distance and closer the angle to linear, the stronger the interaction. The aromatic nature of the catalytic groups, benzyl alcohol and pyridine, also suggest the importance of the π—π and C—H···π types of interactions in stabilizing spiroligozyme conformers; yet, it is difficult to quantify and comment on the energetic stability provided by these interactions.

The three best conformers based on MM evaluation (**D20**, **D34**, and **D35**) have an **Active-H-Bond** QM population above 60%, much higher than that of the parent molecule (8%). For derivatives **D4** and **D31**, on the other hand, density functional theory strongly stabilized the **Inactive-H-Bond** conformers, which constitute more than 90% of the total population.

For **D20**, 24 of 256 conformers have an N···H—O distance less than 3 Å. Of these, 19 overlay excellently with the theozyme and allow a favorable geometry for the acylation reaction. The lowest-energy conformer **D20-1** (Figure 6) constitutes 75% of the total population. **D20-1** is 0.6 kcal mol^{-1} more stable than the lowest-energy **No-H-Bond** conformer (Figure 6, **D20-3**, 16% individual QM population) and 5.7 kcal mol^{-1} compared to the lowest-energy **Inactive-H-Bond** conformer (Figure 6, **D20-2**, 0% individual QM population).

Density functional theory predicts **D34** as the most promising derivative. Of 251 conformers, 13 display $d_{N\cdots H-O}$ < 3 Å, 6 of which have an exposed oxygen nucleophile. **D34-1** is strongly stabilized, having an individual QM population of 96%. The lowest-energy **Inactive-H-Bond** conformer (Figure 6, **D34-2**, 0% individual QM population) and the lowest-energy **No-H-Bond** conformer (Figure 6, **D34-3**, 0% individual QM population) are 4.6 kcal mol^{-1} and 2.7 kcal mol^{-1} higher in energy, respectively.

For **D35**, of 204 conformers, 18 have an N···H—O distance below 3 Å, and 12 present a nicely oriented catalytic dyad for acylation. Even though the lowest-energy **Active-H-Bond** conformer, **D35-1**, has 58% individual QM population, **D35-2**, the **Inactive-H-Bond** conformer, is strong competition, being only 0.2 kcal mol^{-1} higher in energy with an individual QM population of 33%. The energy difference between the lowest-energy **Active-H-Bond** and **No-H-Bond** conformers is also as low as 1 kcal mol^{-1}.

3.4 | MD evaluation

In the last step, three of the derivatives were evaluated using MD simulations. The H-bond occupancies calculated from MD trajectories are previously shown to be good indicators of activity of protein catalysts involving H-bond networks.[26] Six replicas were run for each system. To calculate the occupancy of the intramolecular H-bonding interactions in selected spiroligozymes, a distance cut-off of 3.5 Å and an angle cut-off of 120° were applied as suggested by the ptraj module of AMBER 12. That is, MD population of each spiroligozyme describes the percent ratio of frames with $d_{N\cdots H-O}$ < 3.5 Å and 120° < $\theta_{N\cdots H-O}$ < 180° to the total number of frames in the simulation and represented by the cumulation of points in the above-mentioned region in the N···H-O distance-angle scatter plot given for a representative run (Figure 7). MD populations obtained as averages of six replicas are tabulated in Table 3 (see the SI for MD populations of individual simulations).

D34 and **D35** show only slight improvement of the MD population (5% and 6%, respectively) compared to the parent molecule **A**, whereas **D20** displays a much stronger tendency toward the required H-bonding interaction between the catalytic dyad, with a significant increase in the MD population (27%). Time-distance graphs and the snapshot geometries given in Figure 8 indicate that the H-bond between the catalytic dyad in **D20** is disrupted from time to time, mostly due to competing alternative interactions of the alcohol with the backbone amide oxygens; yet, it is reestablished, and the catalytic groups remain in close proximity throughout the simulation.[54]

All calculations using different methodologies suggest **D20** as a promising spiroligozyme derivative with a better-maintained H-bond between the catalytic dyad compared to the parent molecule. **D20** is also attractive due to its ease of accessibility by simply exchanging a five-membered cyclic building block with an analogous six-membered one in synthesis. Finally, to evaluate the catalytic performance of **D20** in an acyl transfer reaction, we calculated the energy profile of the **D20**-catalyzed transesterification reaction between vinyl trifluoromethylacetate and methanol.

3.5 | Energy Profile

In order to assess whether the spiroligozyme derivative predicted to have an improved H-bond occupancy could function as designed, we computed the stationary points along the transesterification pathway of vinyltrifluoromethylacetate catalyzed by **D20**.

The geometries and relative energies of the optimized structures for the **D20**-catalyzed acyl transfer reaction, together with the analogous acylation pathway calculated with the parent spiroligozyme **A** (relative energies in square brackets), are given in Figure 9. The transesterification mechanism starts with the activation of the alcohol nucleophile by abstraction of its proton by pyridine through a proton-shuttle mechanism and the subsequent attack of the nucleophile to the substrate. **TS1** shows a concerted transition state, in which the alcohol is partially deprotonated by pyridine ($d_{O\text{-}H}$ = 1.28 Å, $d_{N\text{-}H}$ = 1.20 Å) and attacks trifluoromethylacetate ($d_{C\text{-}O}$ = 1.66 Å) with an activation barrier of 16.9 kcal mol^{-1}. The activation energy of the analogous transition state located for the acylation of the parent compound **A** is 2.7 kcal mol^{-1} higher ($\Delta G^{\ddagger}$ = 19.6 kcal mol^{-1}) (see the SI), indicative of more facile acylation of **D20** compared to **A**. This transition state leads to a tetrahedral oxyanionic intermediate, which is stabilized by multiple H-bonding interactions in a so-called oxyanion hole in natural enzymes.[50–52] Yet, as **D20** is a bifunctional spiroligozyme with no oxyanion hole motif,

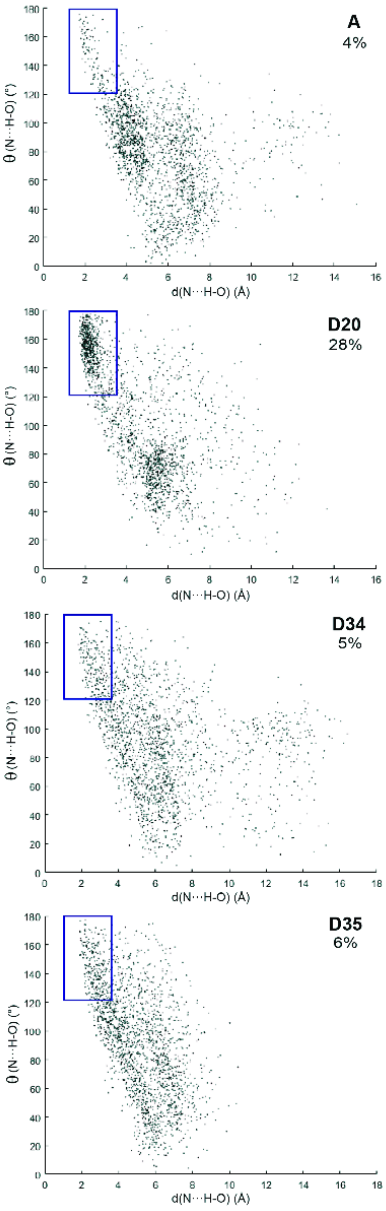

FIGURE 7 N···H—O distance-angle scatter plots and MD populations from MD trajectories of one of the representative replicas

TABLE 3 MD Populations of Selected Derivatives

Derivative no.	MD population (%)
A	4.27 ± 0.85
20	27.3 ± 3.33
34	5.01 ± 1.24
35	5.93 ± 0.76

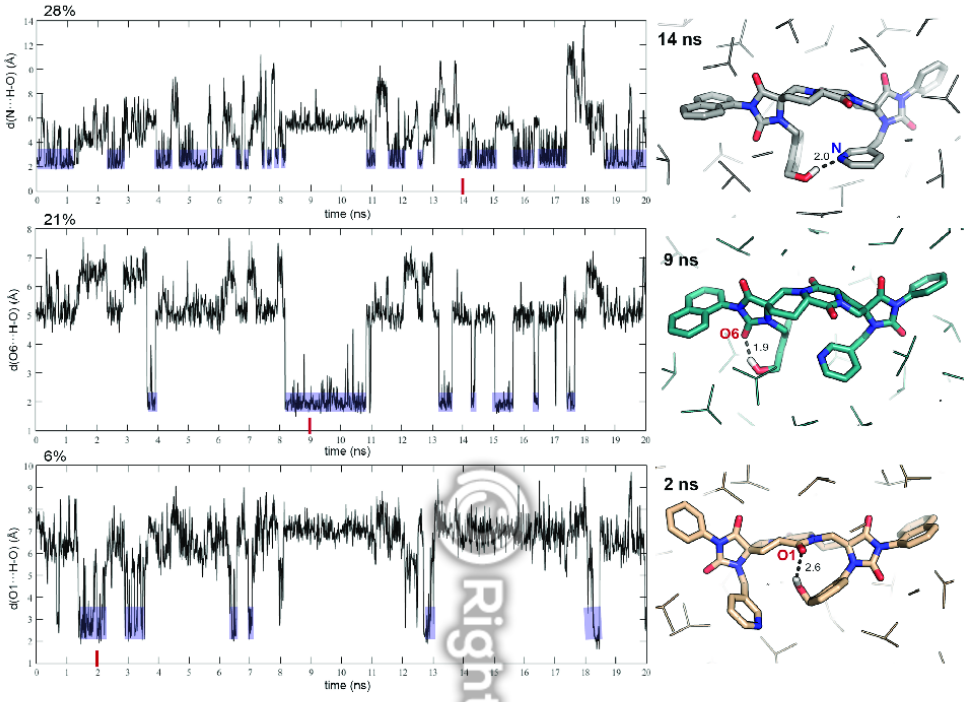

FIGURE 8 Time-distance plots and representative snapshots from the MD simulations for alternative intramolecular interactions in **D20**. Only polar hydrogens are shown for clarity

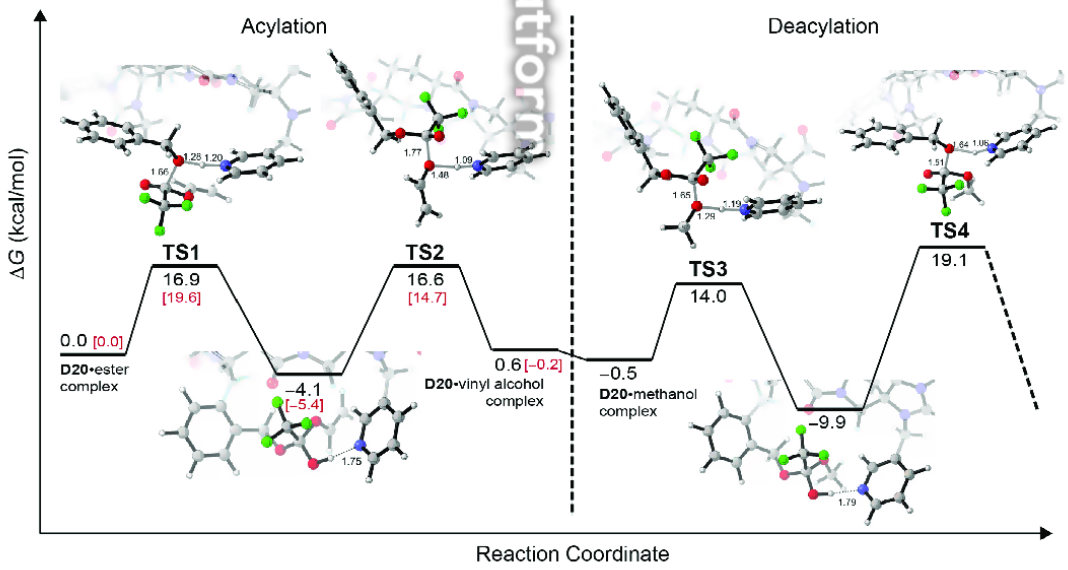

FIGURE 9 Energy profile for the **D20**-catalyzed acyl transfer reaction. Relative energies for the analogous acylation pathway of the parent spiroligozyme **A** are given in square brackets